

# Anti-windup design for input-coupled double integrator systems with application to quadrotor UAV's

Nkemdilim A. Ofodile<sup>a,b,\*</sup>, Matthew C. Turner<sup>a</sup>

<sup>a</sup>*Department of Engineering, University of Leicester, Leicester, UK*

<sup>b</sup>*Air Force Institute of Technology, Kaduna, Nigeria*

---

## Abstract

This paper describes the development of an anti-windup scheme for systems which consist of a parallel set of double integrators preceded by a static coupling element and a saturation nonlinearity. A class of anti-windup compensators are proposed which can guarantee global asymptotic stability of the origin of the closed-loop system. Simple linear-like guidelines for choosing the anti-windup compensator parameters are also given. The anti-windup compensator designs are evaluated on a quadrotor unmanned aerial vehicle. Simulation results and flight tests are presented to demonstrate the effectiveness of this approach.

*Keywords:* Actuator saturation, Aerospace applications, Antiwindup (AW) compensator design, Nonlinear control, Quadrotor unmanned air vehicles (UAVs).

---

## 1. Introduction

The double integrator is a fundamental system in control theory and has attracted great interest from control engineers. Double integrators arise in a great many applications, from mechanical systems (satellites, rigid body motion etc.) to behaviour of agents in network controlled systems [1, 2].

*Saturated* double integrators have also been of interest to researchers studying saturated systems since, it transpires, that they can be globally stabilised by linear feedback control; saturated triple integrators cannot. It suffices to say that saturated control of the double integrator has been studied extensively and  
10 many techniques have been reported in literature [3, 4, 5, 6]. Typically however,

---

\*Corresponding author

*Email addresses:* nao9@leicester.ac.uk, nkofodile@gmail.com (Nkemdilim A. Ofodile), mct6@leicester.ac.uk (Matthew C. Turner)

these studies have been devoted to simple double integrator systems; the class of systems covered in this paper have, to the authors knowledge, not been studied

This paper describes the development of anti-windup compensators for systems which comprise a number of parallel double integrators, preceded by a matrix which effectively introduces coupling between the input channels; preceding this matrix is the saturation nonlinearity which models the actuator constraints - see Figure 1. It is of course possible to use quite standard anti-windup techniques to tackle input saturation in such classes of system and the reader is referred to [7, 8, 9, 10, 11, 12, 13, 14, 15, 16, 17, 18, 19] and references therein for details of these. Furthermore, some specific anti-windup techniques for a class of system which includes that considered here have also been recently proposed by the authors [20, 21].

Many of these techniques provide stability and performance guarantees for the entire nonlinear system by solving a set of linear matrix inequalities (LMIs) [17, 22]. However, for a system of the structure depicted in Figure 1, one would expect that a simpler method could be used to produce a suitable AW compensator. Furthermore, the use of LMIs, would normally generate one “*optimal*” solution whereas there may exist other solutions which might yield an AW compensator with a satisfactory performance. Also, LMI methods typically focus on the  $\mathcal{L}_2$  gain as a performance measure meaning, effectively, that the performance is bounded from above by an affine function of the input energy. However, it may, in fact, not be an adequate measure of the nonlinear system’s performance given the fact that the output energy may scale in a nonlinear way with the input energy in the nonlinear system [23].

The aim of this paper is to develop a globally stabilising anti-windup (AW) scheme for the class of systems described in Figure 1 using the architecture introduced in [14]. The compensators will be parametrised by a state-feedback matrix which is constructed using some intuitive “linear-like” rules and not the  $\mathcal{L}_2$  gain conditions which often prevail in anti-windup synthesis. The approach taken uses the method in [24] which uses a Lure-Postnikov Lyapunov function to generate a Popov-like sufficient condition to guarantee closed-loop global stability for the system.

This solution provides a very large set of stabilising anti-windup compensators for the constrained input-coupled double integrator system. To choose a particular compensator from this set, we advocate the use of formulae based on a simple linear approximation of the compensator’s dynamics. This approach provides a rapid, transparent method for anti-windup design and re-design and offers a level of simplicity and flexibility that will be highly appreciated in a practical environment.

The paper is organised as follows. Section II describes the class of systems under consideration and briefly introduces the anti-windup architecture used. Section III describes the main results of the paper, including the anti-windup design approach and the tuning rules. Section IV introduces the quadrotor platform and presents both simulated and experimental results, and the final section gives

a brief conclusion.

**Notation:** The saturation function is defined as  $\text{sat}(\cdot) : \mathbb{R}^m \mapsto \mathbb{R}^m$  for  $u = [u_1, \dots, u_m]$  and  $u_i > 0, i \in I[1, m]$  such that

$$\begin{aligned} \text{sat}(u) &= [\text{sat}(u_1), \dots, \text{sat}(u_m)]^T \\ \text{sat}(u_i) &= \min\{|u_i|, \bar{u}_i\} \times \text{sign}(u_i) \end{aligned}$$

The deadzone function  $\text{Dz}(\cdot) : \mathbb{R}^m \mapsto \mathbb{R}^m$  is simply

$$\text{Dz}(u) = [\text{Dz}(u_1), \dots, \text{Dz}(u_m)]^T = u - \text{sat}(u) \quad (1)$$

For brevity, we denote  $\tilde{u} = \text{Dz}(u)$ , the notation  $\text{He}\{A\} = A + A^T$ .

$\mathbf{P}^m$  set of  $m \times m$  symmetric positive-definite matrices.

$\mathbf{N}^m$  set of  $m \times m$  symmetric non-negative definite matrices.

$\mathbf{D}$  set of diagonal matrices.

## 60 2. Systems under consideration

### 2.1. The nominal system

The system under configuration is depicted in Figure 1 where  $G(s)$  is the nominal plant and  $K(s)$  is the controller. The reference signal is  $r(t)$ , the measurement  $y(t)$  and the controller demand  $u(t)$ . The plant belongs to the family of input-coupled systems with transfer function matrix

$$G(s) = G_D(s)X \quad (2)$$

where  $G_D(s)$  has a block-diagonal structure

$$G_D(s) = \text{blockdiag}(G_1(s), G_2(s), \dots, G_m(s)) \quad (3)$$

and  $X \in \mathbb{R}^{m \times m}$  is a non-singular matrix. Each element in  $G_D(s)$  has double integrator dynamics.  $G_D(s)$  has the state-space realisation

$$G_D(s) \sim \left[ \begin{array}{c|c} A_D & B_D \\ \hline C_D & D_D \end{array} \right] \quad (4)$$

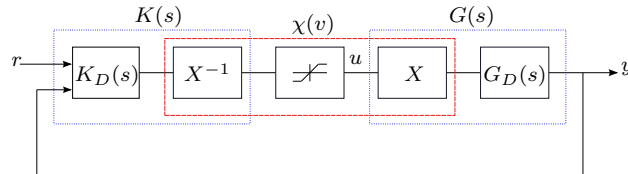


Figure 1: System under consideration

where

$$A_D = \text{blockdiag}(A, A, A, \dots A) \in \mathbb{R}^{2m \times 2m} \quad (5)$$

$$B_D = \text{blockdiag}(B, B, B, \dots B) \in \mathbb{R}^{2m \times m} \quad (6)$$

$$C_D = \text{blockdiag}(C_1, C_2, C_3, \dots C_m) \in \mathbb{R}^{p \times 2m} \quad (7)$$

$$D_D = 0 \quad (8)$$

The matrices  $C_i$  are not restricted to have a particular structure apart from the fact that  $(C_i, A)$  should be detectable for all  $i \in \{1, \dots, m\}$ . The controller  $K(s)$  has the form

$$K(s) = X^{-1}K_D(s) \quad (9)$$

where  $K_D(s)$  has a block diagonal structure compatible with that of  $G_D(s)$ , viz

$$K_D(s) = \text{blockdiag}(K_1(s), K_2(s), \dots, K_m(s)) \quad (10)$$

In the absence of saturation, it is assumed that the controller  $K(s)$  internally stabilises  $G(s)$  and ensures the system exhibits good performance. This is equivalent to  $K_D(s)$  internally stabilising  $G_D(s)$  and, due to their block diagonal structure, this is equivalent to each  $K_i(s)$  internally stabilising  $G_i(s)$  for all  $i \in \{1, \dots, m\}$ . Thus each  $K_i(s)$  can be designed purely on the basis of  $G_i(s)$ .

When saturation is absent, there is no coupling between the  $i$  channels because the nonlinearity (see Figure 1).

$$\chi(v) = X \text{sat}(X^{-1}v) \quad (11)$$

is simply the identity operator. However, when saturation is present i.e  $\chi(v) \neq v$ , the saturation element causes some nonlinear coupling between the system's  $m$  control loops and, unless  $X$  is diagonal, the decoupling offered by the nominal controller (10) is lost. This coupling is a well known trigger for performance deterioration and instability [25].

## 2.2. Anti-windup compensator architecture

While a number of different anti-windup approaches [10] could be used to tackle the saturation problem described above, these would typically produce an *unstructured* anti-windup compensator. This section introduces a specially structured anti-windup compensator which exploits the structure of the plant (2) and controller (9). The approach used is based on that introduced in [20, 21].

Consider the system depicted in Figure 2 where  $K(s)$  and  $G(s)$  are the structured plant and controller described in equations (2), (9), (4) and (10). Again,  $r(t)$  is the reference,  $y(t)$  the output and  $u(t)$  the physical control input. Also shown is  $v(t)$  which can be considered as the *virtual* control input and the anti-windup compensator  $\Theta(s)$ . The plant has a state-space realisation

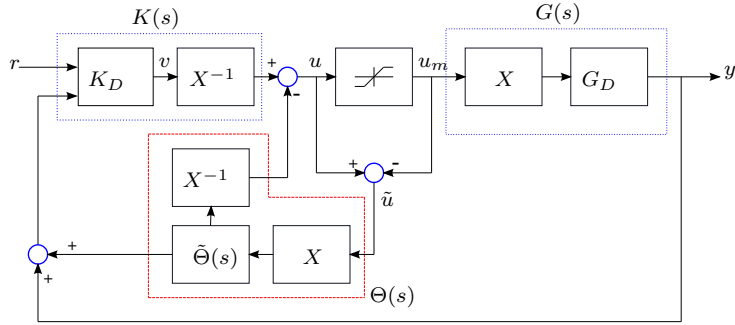


Figure 2: Input-coupled system with structured anti-windup

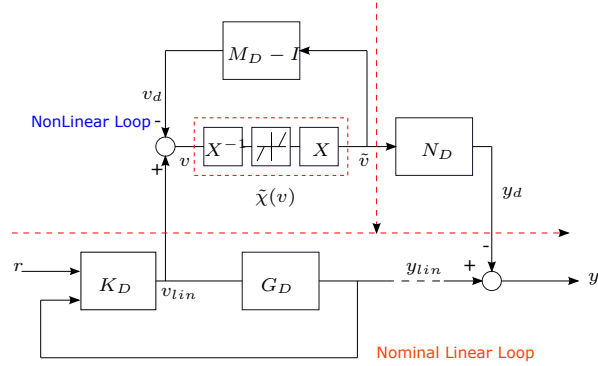


Figure 3: Equivalent interpretation of structured anti-windup problem

$$G(s) \sim \begin{cases} \dot{x} &= A_D x + B_D X u_m \\ y &= C_D x \end{cases} \quad (12)$$

where  $u_m = \text{sat}(u)$  and the controller has the realisation

$$K(s) \sim \begin{cases} \dot{x}_c &= A_c x_c + B_{cr} r + B_{cy} (y + y_d) \\ v &= C_c x_c + D_{cr} r + D_{cy} (y + y_d) \\ u &= X^{-1} (v - v_d) \end{cases} \quad (13)$$

Following [21], the anti-windup compensator is given the following structure,

$$\Theta(s) \sim \begin{cases} \dot{x}_a &= (A_D + B_D F_D) x_a + B_D X (u - u_m) \\ v_d &= F_D x_a \\ y_d &= C_D x_a \end{cases} \quad (14)$$

where the, yet-to-be-defined matrix  $F_D$  has the following structure.

$$F_D = \text{blockdiag}(F_1, F_2, \dots, F_m) \quad (15)$$

The anti-windup compensator dynamics (14) are structured compatibly with those of the plant dynamics  $G_D(s)$ . In fact, the anti-windup compensator has a coprime-factor based structure [21, 14] although this will not be important here. Defining  $e = x + x_a$ , it follows that the dynamics (12)-(14) can be written

90 as

$$G_{cl}(s) \sim \begin{cases} \dot{e} &= (A_D + B_D D_{cy} C_D)e + B_D C_c x_c + B_D D_{cr} r \\ \dot{x}_c &= B_{cy} C_D e + A_c x_c + B_{cr} r \\ v_{lin} &= D_{cy} C_D e + C_c x_c + D_{cr} r \\ y_{lin} &= C_D e \end{cases} \quad (16)$$

$$\Theta(s) \sim \begin{cases} \dot{x}_a &= (A_D + B_D F_D)x_a + B_D \tilde{\chi}(v_{lin} - v_d) \\ v_d &= F_D x_a \\ y_d &= C_D x_a \end{cases} \quad (17)$$

where  $\tilde{\chi}(\cdot) : \mathbb{R}^m \mapsto \mathbb{R}^m$  is defined as

$$\tilde{\chi}(v) := XDz(X^{-1}v) = v - \chi(v) \quad (18)$$

Graphically, this implies that Figure 2 can be re-drawn as Figure 3. This prompts the following standing assumption.

**Assumption 1.** *The following matrix is Hurwitz*

$$A_{cl}(s) = \begin{bmatrix} A_D + B_D D_{cy} C_D & B_D C_c \\ B_{cy} C_D & A_c \end{bmatrix}$$

With this assumption in mind, one can then see from the dynamics (16) and (17), or equivalently from Figure 3 that the entire system will be stable, if the upper block is stable, or equivalently if the origin of (17) is asymptotically stable. The main stability problem in the paper can now be defined.

100 **Problem 1.** *Consider the system (17) where  $A_D, B_D, C_D$  are defined in (5)-(7),  $\tilde{\chi}(\cdot) : \mathbb{R}^m \mapsto \mathbb{R}^m$  is defined in (18) and  $X$  is a nonsingular matrix. Find conditions on  $F_D$  which ensure the origin is globally asymptotically stable.*

A similar problem was considered in [20, 21], but in that paper, it was assumed that the plant was strictly stable,  $G_i(s) \in \mathcal{RH}_\infty$  for all  $i \in \{1, \dots, m\}$ . It is easy to relax the conditions in [21] to the case that  $G(s) \notin \mathcal{RH}_\infty$  (as is the case here), but then the results provided are only local not global. In the next section, global results will be provided.

### 3. Structured Anti-windup design

Section 2.1 established that, with the structure of anti-windup compensator given in equation (14), the stability of the system in Figure 2 is equivalent to that in Figure 3. Under Assumption 1, the stability of Figure 2 is then reduced to that of finding an  $F_D$  which guarantees the stability of the origin of the system described in equation (17). This section will provide a family of matrices  $F_D$  which solve Problem 1 and will give guidance on how one might select a particular  $F_D$  from this family.

#### 3.1. Tyan and Bernstein's Result

Consider a linear system with input saturation whose state-space realization is given as;

$$\dot{x}(t) = A_o x(t) + B_o \text{sat}(u(t)) \quad (19)$$

$$u(t) = K_o x(t) \quad (20)$$

where it is assumed that the state-space matrices are structured as

$$A_o = \begin{bmatrix} A_z & 0 \\ 0 & A_s \end{bmatrix} \quad B_o = \begin{bmatrix} B_z \\ B_s \end{bmatrix} \quad (21)$$

$A_s \in \mathbb{R}^{n_s \times n_s}$  is Hurwitz,  $A_z \in \mathbb{R}^{n_z \times n_z}$  and has eigenvalues on the imaginary axis.  $B_z \in \mathbb{R}^{n_z \times m}$ ,  $B_s \in \mathbb{R}^{n_s \times m}$  and all signals are assumed to be of compatible dimensions.

According to [24], it is possible to present sufficient conditions which ensure global stability of the above system by using a Popov-like Lyapunov function that consists of a positive *semi*-definite quadratic term and an additional integral term. This result is summarized as follows;

**Theorem 1.** *Given that*

$$R = \begin{bmatrix} R_z & 0 \\ 0 & R_s \end{bmatrix}, \quad R_z \in \mathbf{N}^{n_z}, \quad R_s \in \mathbf{N}^{n_s}, \quad K_o = [K_1 \dots K_m]^T$$

*and assuming that  $(A_o, K_o)$  is observable or  $(A_o, K_o)$  is detectable and  $(A_o, R)$  is observable, if there exist matrices  $R_2 \in \mathbf{DN}^{n_z}$ ,  $N \in \mathbf{DN}^{n_s}$ ,  $P \in \mathbf{N}^{(n_z+n_s)}$  such*

that the following equations and inequalities are satisfied:

$$0 = A_o^T P + P A_o + R \quad (22)$$

$$0 = B_o^T P + N K_o A_o + R_2 K_o \quad (23)$$

$$0 < 2R_2 - (N K_o B_o + B_o^T K_o^T N) \quad (24)$$

$$0 < P + K_o^T N K_o \quad (25)$$

then the origin of the system (19)-(20) is globally asymptotically stable and the Lyapunov function guaranteeing stability is given by

$$V(x) = x^T P x + 2 \sum_{i=1}^m \int_0^{u_i = K_i x} N_i \text{sat}_i(u_i) du_i$$

The proof of Theorem 1 can be found in [24]. The proof shows that global stability can be guaranteed for the given saturated system in (19)-(20) or used to construct a stabilizing controller for the system. This result is used in the next two sections as the basis for constructing anti-windup compensators. The main novelty of this result is that there is no requirement for the quadratic part of the Lyapunov function to be positive definite; only positive *semi*-definiteness of this is required. This enables relaxed conditions for global asymptotic stability to be obtained, compared to those normally obtained using Lur'e Lyapunov functions.

### 3.2. Anti-windup design for input-coupled double integrator systems

This section applies Theorem 1 to the structured anti-windup design problem, defined in Problem 1. In order to study asymptotic stability of the origin, note that the state-equation in (17) can be re-written, in the case where  $v_{lin} \equiv 0$ , as

$$\dot{x}_a = A_D x_a + B_D X \text{sat}(X^{-1} F_D x_a) \quad (26)$$

which is in the same form as in Theorem 1, with  $A_z = A_D$ ,  $B_z = B_D$  and  $K = F_D$ . The following proposition is the main result of the section.

**Proposition 1.** Consider the system (17) where  $A_D, B_D, C_D$  are defined in (5)- (7),  $\tilde{\chi}(\cdot) : \mathbb{R}^m \mapsto \mathbb{R}^m$  is defined in (18) and  $X \in \mathbb{R}^{m \times m}$  is a nonsingular matrix. Assume that there exists two positive definite diagonal matrices  $V$  and  $W$  such that

$$V = X^T W X$$

and let  $F_D = (I_m \otimes F)$  where  $F = [F_a \ F_b]$  is chosen such that  $\text{sign}(F_a) = \text{sign}(F_b) = -\text{sign}(\beta)$ . Then the origin of (17) is globally asymptotically stable.

**Proof:** This proof is an application of Theorem 1 to the system (26). In this case,  $A_z = A_D$ ,  $B_z = B_D$  and  $K = F_D$ , so equations/inequalities (22)-(25) become:

$$0 = A_D^T P_D + P_D A_D + R_z \quad (27)$$

$$0 = X^T B_D^T P_D + N X^{-1} F_D A_D + R_2 X^{-1} F_D \quad (28)$$

$$0 < 2R_2 - N X^{-1} F_D B_D X + X^T B_D^T F_D^T (X^{-1})^T N \quad (29)$$

$$0 < P_D + F_D^T (X^{-1})^T N X^{-1} F_D \quad (30)$$

Let  $R_z = 0$  and  $R_2 = 0$ , (this satisfies the conditions of Theorem 1 i.e  $R_z, R_2 \in \mathbb{D}^m \geq 0$ ) and let  $N = V$  where  $V$  is a positive definite diagonal matrix which therefore also satisfies the conditions of Theorem 1 ( $N \in \mathbb{D}^m \geq 0$ ). This implies that the expressions (27) - (30) become

$$0 = A_D^T P_D + P_D A_D \quad (31)$$

$$0 = X^T B_D^T P_D + V X^{-1} F_D A_D \quad (32)$$

$$0 < -V X^{-1} F_D B_D X + X^T B_D^T F_D^T (X^{-1})^T V \quad (33)$$

$$0 < P_D + F_D^T (X^{-1})^T V X^{-1} F_D \quad (34)$$

By assumption  $V = X^T W X$  for diagonal positive definite  $V, W$ , so  $W = (X^T)^{-1} V X^{-1}$ . Letting  $P_D = W \otimes P$  where  $P \in \mathbb{R}^{2 \times 2} \geq 0$ , means that (31) - (34) can be re-written as

$$0 = (I_m \otimes A^T)(W \otimes P) + (W \otimes P)(I_m \otimes A) \quad (35)$$

$$0 = X^T (I_m \otimes B^T)(W \otimes P) + V X^{-1} (I_m \otimes F)(I_m \otimes A) \quad (36)$$

$$0 < -V X^{-1} (I_m \otimes F)(I_m \otimes B) X + X^T (I_m \otimes B^T)(I_m \otimes F^T)(X^{-1})^T V \quad (37)$$

$$0 < (W \otimes P) + (I_m \otimes F^T)(X^{-1})^T V X^{-1} (I_m \otimes F) \quad (38)$$

Using the following properties

$$(A \otimes B)(C \otimes D) = AC \otimes BD \quad (39)$$

$$(A \otimes B)^T = A^T \otimes B^T \quad (40)$$

equations 35- 38 then simplify to:

$$0 = W \otimes (P A^T + P A) \quad (41)$$

$$0 = X^T (W \otimes (B^T P + F A)) \quad (42)$$

$$0 < -X^T (W \otimes (F B + B^T F^T)) X \quad (43)$$

$$0 < W \otimes (P + F^T F) \quad (44)$$

Next, each expression (41)-(44) is considered in turn. Let  $A$  and  $B$  have the realisations

$$A = \begin{bmatrix} 0 & 1 \\ 0 & 0 \end{bmatrix} \quad B = \begin{bmatrix} 0 \\ \beta \end{bmatrix} \quad (45)$$

<sup>150</sup> **Equation 41.** Because  $W$  is positive definite by assumption, this holds if  $A^T P + PA = 0$ . Letting

$$P = \begin{bmatrix} P_a & P_b \\ P_b & P_d \end{bmatrix} \quad (46)$$

we thus have

$$\begin{bmatrix} 0 & 0 \\ 0 & 0 \end{bmatrix} = \begin{bmatrix} 0 & 1 \\ 0 & 0 \end{bmatrix}^T \begin{bmatrix} P_a & P_b \\ P_b & P_d \end{bmatrix} + \begin{bmatrix} P_a & P_b \\ P_b & P_d \end{bmatrix} \begin{bmatrix} 0 & 1 \\ 0 & 0 \end{bmatrix} \quad (47)$$

$$= \begin{bmatrix} 0 & 0 \\ P_a & P_{b/c} \end{bmatrix} + \begin{bmatrix} 0 & 0 \\ P_a & P_{b/c} \end{bmatrix}^T \quad (48)$$

Therefore  $P_a = P_b = 0$ .

**Equation 42.**  $X$  is full rank, so this holds if  $B^T P + F^T A = 0$ . This is equivalent to

$$\begin{bmatrix} 0 & 0 \end{bmatrix} = \begin{bmatrix} 0 & \beta \end{bmatrix} \begin{bmatrix} P_a & P_b \\ P_b & P_d \end{bmatrix} + \begin{bmatrix} F_a & F_b \end{bmatrix} \begin{bmatrix} 0 & 1 \\ 0 & 0 \end{bmatrix} \quad (49)$$

$$= \begin{bmatrix} \beta P_b & \beta P_d + F_a \end{bmatrix} \quad (50)$$

Therefore  $P_d = -F_a/\beta$  and because,  $P_d$  must be positive semi-definite it is necessary and sufficient for  $\text{sign}(F_a) = -\text{sign}(\beta)$  or  $P_d = 0$  and  $F_a = 0$ .

**Inequality 43.** Again noting that  $X$  is full rank, this is satisfied if  $-FB - B^T F^T > 0$ . This can be written as

$$0 < - \begin{bmatrix} F_a & F_b \end{bmatrix} \begin{bmatrix} 0 \\ \beta \end{bmatrix} + \begin{bmatrix} 0 & \beta \end{bmatrix} \begin{bmatrix} F_a \\ F_b \end{bmatrix} \quad (51)$$

$$= -2F_b\beta \quad (52)$$

Thus for this inequality to hold we must have  $\text{sign}(F_b) = -\text{sign}(\beta)$ .

**Inequality 44.** Finally, noting that  $P_a = P_b = 0$ , inequality (44) holds if

$$0 < \begin{bmatrix} 0 & 0 \\ 0 & P_d \end{bmatrix} + \begin{bmatrix} F_a \\ F_b \end{bmatrix} \begin{bmatrix} F_a & F_b \end{bmatrix} = \begin{bmatrix} F_a^2 & F_a F_b \\ F_a F_b & P_d + F_b^2 \end{bmatrix} \quad (53)$$

Therefore for this inequality to hold we must strengthen our conclusion to  $\text{sign}(F_a) = -\text{sign}(\beta)$ : it cannot be zero or only positive semi-definiteness would be proven.

Hence with  $\text{sign}(F_a) = \text{sign}(F_b) = -\text{sign}(\beta)$ , the conditions of Theorem 1 are fulfilled and the origin of the system (26) will be globally asymptotically stable.  $\square$

This proposition proves that for input-coupled double integrator systems, there exist a large family of anti-windup compensators which are able to ensure global asymptotic stability of the origin.

**Remark 1:** Note that in the case that  $X = 1$  and hence  $\chi(\cdot) = \text{sat}(\cdot)$ , the system (26) reduces to the simple saturated double integrator system which was discussed in [24, 26]

### 3.3. Performance Consideration

Proposition 1 shows that for input-coupled double integrator plants, there exist a large family of anti-windup compensators guaranteeing global asymptotic stability: the entries of the matrix  $F$  simply need to be opposite in sign to  $\beta$ . However, only a portion of this range of values may provide acceptable *performance*. In this section, we propose a transparent procedure for selecting suitable ranges of  $F$  for acceptable performance based on the anti-windup compensator dynamics.

Due to the structure of the anti-windup compensator, the plant and the controller, the gains  $F$  are chosen on a loop-by-loop basis; that is the standard double integrator system is considered in order to choose the gains of  $F$ , which is then used to construct  $F_D = (I \otimes F)$  as required for the full anti-windup dynamics given in (14). Therefore, we set  $m = 1$  and consider the anti-windup dynamics given by equation (26) which can be written as

$$\dot{x} = Ax + B\text{sat}(u) \quad u = Fx \quad (54)$$

The saturation function is then replaced by the time varying gain, viz:

$$\text{sat}(u) = \sigma(u)u \quad \sigma(\cdot) : \mathbb{R} \mapsto [0, 1] \quad (55)$$

This then results in

$$\dot{x} = (A + B\sigma(u)F)x \quad (56)$$

The  $A$ -matrix of the compensator therefore has the form

$$A + B\sigma(u)F = \begin{bmatrix} 0 & 1 \\ \beta\sigma(u)F_a & \beta\sigma(u)F_b \end{bmatrix} \quad (57)$$

We can use simple linear analysis to estimate the performance of the AW compensator since it is known that any  $F$  satisfying Proposition 1 will ensure global

stability of the origin. Hence, the roots of the characteristic equation for the nonlinear loop will remain inside the desired stability region and the characteristic equation is given by

$$s^2 - \beta\sigma(u)F_b s - \beta\sigma(u)F_a = 0 \quad (58)$$

If  $\sigma(u)$  is replaced by a constant  $\sigma_0$  such that  $\sigma_0 \in [0, 1]$  then the above equation becomes

$$s^2 - \beta\sigma_0 F_b s - \beta\sigma_0 F_a = 0 \quad (59)$$

The standard second order characteristic equation is defined as

$$s^2 + 2\zeta\omega_n s + \omega_n^2 = 0 \quad (60)$$

where  $\omega_n$  is the undamped natural frequency and  $\zeta$  is the damping ratio. Thus comparing the coefficients of both equations 59 and 60, we can obtain expressions for  $\omega_n$  and  $\zeta$  as

$$\omega_n = \sqrt{-\beta\sigma_0 F_a} \quad \zeta = -\frac{F_b}{2} \sqrt{-\frac{\beta\sigma_0}{F_a}} \quad (61)$$

Rearranging equation (61) such that  $F_a$  and  $F_b$  are made subject of the formula gives

$$F_a = -\omega_n^2 / \beta\sigma_0 \quad F_b = -2\zeta \sqrt{-\frac{F_a}{\beta\sigma_0}} \quad (62)$$

Equation (62) implies that  $F_a$  is a function of the desired natural frequency  $\omega_n$  of the system while  $F_b$  is a function of the selected value of  $F_a$  and the desired damping ratio  $\zeta$ . Note however that both  $F_a$  and  $F_b$  depend also on  $\sigma_0$  which represents the level of saturation. In reality, the saturation level varies, causing  $\sigma_0$  to fluctuate between the range  $[0, 1]$ . However,  $F_a$  and  $F_b$  could be designed by choosing a suitable value of  $\sigma_0$ , possibly corresponding to some lower limit on  $\sigma$  and then it would be expected that the compensators would have acceptable performance if the saturation did not cause  $\sigma(\cdot)$  to deviate too much from this value. For example, if the control signal was expected to exceed twice the saturation limits,  $\sigma_0$  could be chosen as 0.5 and hence, the AW compensator can be designed using this value. This means that for each fixed  $\sigma(u) \in [0, \sigma_0]$ , the anti-windup compensator would then have a damping ratio of no greater than the  $\zeta$  associated with  $\sigma(u) = \sigma_0$ . It is accepted that this approach will not guarantee any rigorous performance specification, but it seems to work well in the practical results reported later.

## 4. Quadrotor UAV Simulation and Experimental Results

### 4.1. Quadrotor platform description

The quadrotor UAV has emerged as an interesting aerial platform for a number of useful applications. It has been the subject of several studies [27, 28, 29, 21] including the problem of saturation in UAVs [30, 31, 21, 32].



Figure 4: Picture of the 2014 3DR Quadrotor

The 2014 3DR quadrotor [33] is used as an experimental platform in this paper (see Figure 4). It is a DIY quadrotor kit that has been equipped with a variety of sensors onboard including the inertial measurement unit-IMU (3-axes accelerometers and rate gyroscopes), magnetometers and barometric pressure sensors. These sensors are contained in the Ardupilot Mega (APM 2.6) programmable flight controller board whose firmware has been modified to suit our design requirements.

This quadrotor consists of a number of components which include four 850kV brushless DC motors, four 12" two-bladed propellers, a 4in1 20A electronic speed controller (ESC), a GPS-compass system, a Lithium-polymer 11.1V, 5500mAh battery and a 433MHz transceiver telemetry kit. The interconnection of all these components is shown in Figure 5. The quadrotor performance and status is monitored from a computer that runs the software that communicates with the quadrotor remotely via the telemetry system. The values of the controller gains as well as other important parameters of the 3DR quadrotor are given in the Table 1. The next subsection describes the generated forces and torques as applied to the dynamics of the quadrotor UAV.

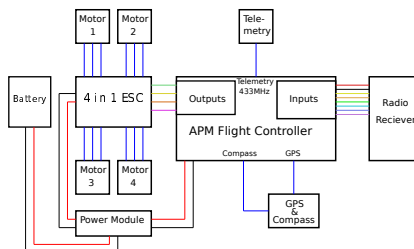


Figure 5: Quadrotor hardware schematic

#### 4.2. Dynamic Model

The model of the quadrotor used for design and simulation is similar to that developed in [34]. Consider the structure of a quadrotor UAV as depicted in Figure 6. Each motor acts on the body depending on its varying rotational

Table 1: Approximate values of 3DR Quadrotor parameters and online PD Gains

Parameters	Description	Values	Units
$g$	Gravity	9.81	$ms^{-2}$
$m$	Mass	2.1	$kg$
$d$	Distance	0.3	$m$
$k_1$	Force constant	0.89	
$k_2$	Torque constant	0.11	
$J_x$	Pitch Inertia	$2.85 \times 10^{-6}$	$kgm^{-2}$
$J_y$	Roll Inertia	$2.85 \times 10^{-6}$	$kgm^{-2}$
$J_z$	Yaw Inertia	$1.81 \times 10^{-6}$	$kgm^{-2}$
$K_{\phi,P}$	Proportional gain	0.22	
$K_{\theta,P}$		0.22	
$K_{\psi,P}$		0.4	
$K_{\phi,D}$	Derivative gain	0.004	
$K_{\theta,D}$		0.004	
$K_{\psi,D}$		0.003	
Throttle via $K_{z,P}$	Throttle rate P gain	6	
Throttle via $K_{z,D}$	Throttle rate D gain	0.001	

speed and generates an input force and a torque as it rotates. The total sum of all the forces generated by the motors control the lift force. The four motors can be thought of as two pairs, for which one pair of motors (front and back motors) rotating in one direction control the pitch  $\theta$  and the other pair of motors (left and right motors) rotating in the opposite direction control the roll  $\phi$  while a manipulation of the speed of both pairs control the yaw  $\psi$  movement.

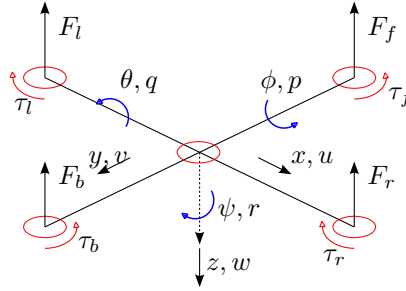


Figure 6: Schematic showing Force, Torque and States definition of a Quadrotor

The full nonlinear dynamic model was constructed according to [34] and was used for simulation purposes. For controller and anti-windup compensator design, the model was simplified according to that procedure described in [34]. In

particular, the dynamics of the quadrotor can be summarised as

$$\begin{cases} \ddot{\phi} &= \frac{1}{J_x} \tau_\phi \\ \ddot{\theta} &= \frac{1}{J_y} \tau_\theta \\ \ddot{\psi} &= \frac{1}{J_z} \tau_\psi \\ \ddot{z} &\approx g - \frac{1}{m} F \end{cases} \quad (63)$$

where  $\phi, \theta$  and  $\psi$  are the pitch, roll and yaw attitudes in inertial space,  $J_x, J_y, J_z$  are the moments of inertia in the  $x, y, z$  axes,  $\tau_\phi, \tau_\theta, \tau_\psi$  are the roll pitch and yaw torques,  $F$  is the total lift force and  $m, g$  are the mass of the quadrotor and acceleration due to gravity respectively. Note that the dynamics are, essentially a set of parallel integrators with transfer function matrix

$$G_D(s) = \text{diag}\left(\frac{1}{J_x s^2}, \frac{1}{J_y s^2}, \frac{1}{J_z s^2}, \frac{1}{m s^2}\right) \quad (64)$$

The relationship between the physical control signal, which is taken as the square of the motor velocities, and the body axis torques and forces are given [34] as

$$\begin{bmatrix} F \\ \tau_\phi \\ \tau_\theta \\ \tau_\psi \end{bmatrix} = \underbrace{\begin{bmatrix} k_1 & k_1 & k_1 & k_1 \\ 0 & -\rho k_1 & 0 & \rho k_1 \\ \rho k_1 & 0 & -\rho k_1 & 0 \\ -k_2 & k_2 & -k_2 & k_2 \end{bmatrix}}_X \underbrace{\begin{bmatrix} \delta_f \\ \delta_r \\ \delta_b \\ \delta_l \end{bmatrix}}_u \quad (65)$$

where  $k_1$  and  $k_2$  are constants that are determined experimentally,  $\rho$  is the distance between the centre of mass and the propellers, and  $\delta_*$  is the motor angular velocity squared. Thus the linearised quadrotor dynamics have the form  $G(s) = G_D(s)X$  as required.

Because  $X$  is invertible, the controller for the system will take the form;  $K(s) = X^{-1}K_D(s)$  where  $K_D(s)$  is a block diagonal transfer function matrix, as indicated in equation (10) with each element consisting of a PD controller for each individual channel. The diagonal elements of the controller  $K_D(s)$  therefore have the form

$$K_D(s) \sim \begin{cases} v_\phi &= K_{\phi,P}[r_\phi - \phi] - K_{\phi,D}[p] \\ v_\theta &= K_{\theta,P}[r_\theta - \theta] - K_{\theta,D}[q] \\ v_\psi &= K_{\psi,P}[r_\psi - \psi] - K_{\psi,D}[r] \\ v_z &= K_{z,P}[r_z - z] - K_{z,D}[\dot{z}] + g \end{cases} \quad (66)$$

where  $K_{\phi,P}, K_{\theta,P}, K_{\psi,P}, K_{z,P}$  are the proportional gains,  $K_{\phi,D}, K_{\theta,D}, K_{\psi,D}, K_{z,D}$  are the derivative gains,  $v_{\phi,\theta,\psi,z}$  is the control input (in virtual coordinates),  $r_{\phi,\theta,\psi,z}$  is the desired reference,  $p, q, r$  are the angular rates corresponding to  $\dot{\phi}, \dot{\theta}, \dot{\psi}$  and  $\phi, \theta, \psi, z$  is the system output. There is a slight abuse of notation in equation (64) since the height controller is actually affine with a gravity compensation term included. In the absence of saturation, note that this controller will form a

Table 2: Damping Ratios and AW Gains for Simulations at  $\omega_n = 800rad/s$

Damping Ratio	$F_a$	$F_b$	Remark
$\zeta = 0.5$	-1.8240	-0.0023	$\zeta < 1$
$\zeta = 1$	-1.8240	-0.0046	$\zeta = 1$
$\zeta = 5$	-1.8240	-0.0228	$\zeta > 1$

Table 3: Damping Ratios and AW Gains for Simulations at  $\omega_n = 500rad/s$

Damping Ratio	$F_a$	$F_b$	Remark
$\zeta = 0.5$	-0.7125	-0.0014	$\zeta < 1$
$\zeta = 1$	-0.7125	-0.0028	$\zeta = 1$
$\zeta = 5$	-0.7125	-0.0142	$\zeta > 1$

set of 4 decoupled closed-loops where each controller stabilises one of the double integrator systems. However, note that when saturation occurs, this decoupling is compromised and performance deterioration occurs.

The dynamics of the quadrotor (64) can be written in the form of (3) by choosing a state-space realisation where  $A_D$  has the form in (5) and  $B_D$  has the form in (6) with  $\beta = 1$ . This then implies  $C_D$  has the form of (7) where  $m = 4$  and

$$C_1 = \frac{1}{J_x} I_2 \quad C_2 = \frac{1}{J_y} I_2 \quad C_3 = \frac{1}{J_z} I_2 \quad C_4 = \frac{1}{m} I_2 \quad (67)$$

This, coupled with the fact that there exists diagonal positive definite matrices  $W, V$  such that  $V = X^T W X$ , enables the design of anti-windup compensators according to Section 3.3.

#### 250 4.3. Simulation Results

AW compensators corresponding to the approach described above were designed for the entire quadrotor system at  $\sigma_0 = 1$ . The AW compensators had a natural frequency of  $\omega_n = 800rad/s$  and the damping ratio was varied as listed in Table 2. A further set of AW compensators were designed using a frequency of  $\omega_n = 500rad/s$  and the damping ratio was varied as listed in Table 3. For brevity, only the pitch responses are discussed here.

Figure 7a shows the nominal response of the pitch channel for a pulse demand of  $0.4rad$  and Figure 7b indicates that the saturated system has poor performance and displays overshoot several times greater than the attitude demand. During

260 saturation, some off-axis coupling can be observed (not shown on plot) because the system loses the decoupling properties provided by virtue of the structure  $G(s) = G_D(s)X$ .

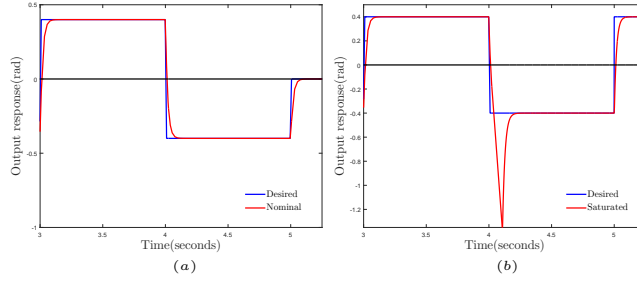


Figure 7: Pitch output response:(a) Nominal; (b) Saturation, no AW

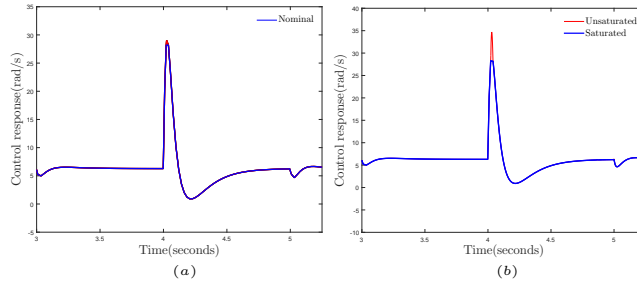


Figure 8: Control response:(a) Nominal; (b) Saturation, no AW

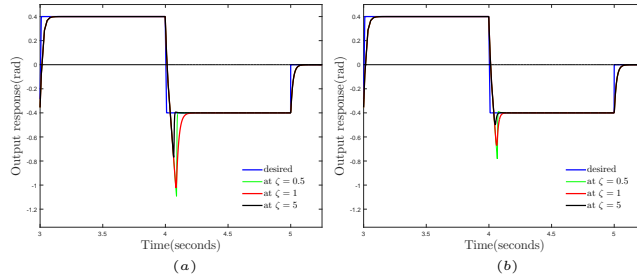


Figure 9: Pitch output response:(a) Saturation,  $\omega_n = 500\text{rad/s}$  with AW at different  $\zeta$ ; (b) Saturation,  $\omega_n = 800\text{rad/s}$  with AW at different  $\zeta$

Figures 9a and 9b show the pitch response with AW compensation. The pitch response improves as  $\zeta$  increases from 0.5 to 5 with the best response at  $\zeta = 5$ . Note that at higher undamped natural frequencies, better responses were obtained from the system and these can be seen in the difference between Figure 9a and Figure 9b. All plots of Figure 8 and Figure 10 show the control signal response both at nominal and at saturation.

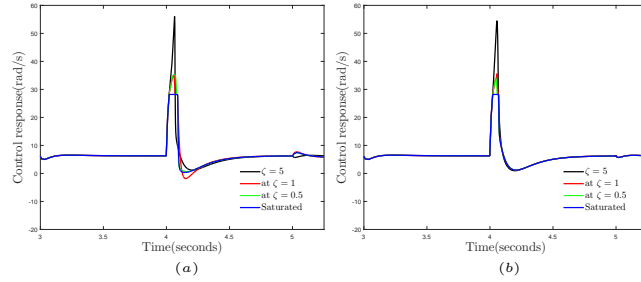


Figure 10: Control response: [(a), (b)] Saturation,  $\omega_n = 500\text{rad/s}$  and  $\omega_n = 800\text{rad/s}$  with AW at different  $\zeta$

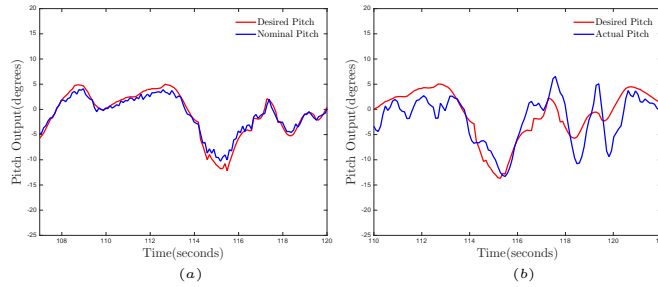


Figure 11: Pitch angle response-Artificial limit flight section: (a) [from left] Typical Nominal response ; (b) Saturated response no AW

#### 4.4. Flight Test Results

270 The quadrotor platform was setup with the PD controller as the baseline controller while simple PID controllers were added as outer-loop controllers for waypoint navigation. The outer loop controllers were used to prepare the UAV for autonomous flight with a constant mission in an outdoor environment. In the outdoor flight, the quadrotor was set up to follow pre defined mission paths and reference commands coded in its autopilot while it was monitored remotely via a telemetry link.

The saturated motor commands are angular velocities but our quadrotor has

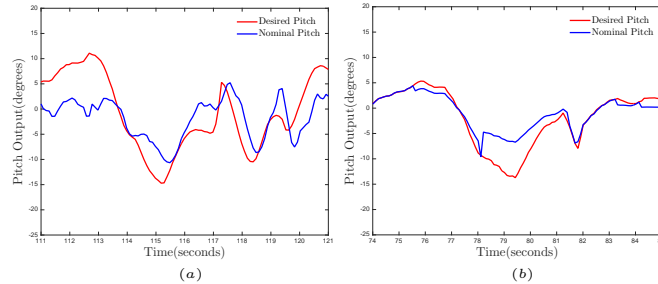


Figure 12: Pitch angle response: (a) [from left] Saturation,  $\omega_n = 500\text{rad/s}$  with AW at  $\zeta = 0.5$ ; (b) Saturation,  $\omega_n = 500\text{rad/s}$  with AW at  $\zeta = 2$ .

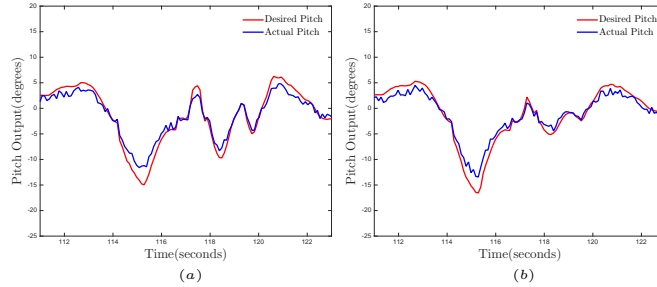


Figure 13: Pitch angle response: (a) [from left] Saturation,  $\omega_n = 840\text{rad/s}$  with AW at  $\zeta = 0.5$ ; (b) Saturation,  $\omega_n = 840\text{rad/s}$  with AW at  $\zeta = 2$ .

no sensor that measures this. However, there is a direct correlation between the angular velocities and the motor's PWM commands; where the angular velocity is obtained by converting the motor velocity data provided in revolutions per minute (RPM) values for pulse width modulation (PWM) levels operating within a range of  $1000 \mu\text{s}$  (1 ms) and  $2000 \mu\text{s}$  (2 ms) at a frequency of 490 Hz. For this system, the motor's PWM values are used as the saturated elements instead of the angular velocities.

The saturation limits on the motor command were imposed on the system using the firmware and were set to a modest 13% of nominal operation. These were done to help maintain a certain level of uniformity in the flight data results collected and to ensure maximum safety.

Figure 11a shows a typical pitch response when no artificial limits were imposed. This can be interpreted as the *nominal case*. Figure 11b shows a similar section of the flight, but with the artificial limits applied, but without AW compensation. One can see that when the limits are imposed, the pitch response deteriorates and almost becomes unstable.

Figures 12a and 12b show the response of the system when the artificial limits are applied and the AW compensators corresponding to  $\omega_n = 500\text{rad/s}$  at  $\zeta = 0.5$  and  $\zeta = 2$  are used. The results seem better than the saturated no AW case but with a less than desirable signal tracking.

Figures 13a and Figure 13b show improved responses when the artificial limits are applied and the AW compensators corresponding to  $\omega_n = 840\text{rad/s}$  at  $\zeta = 0.5$  and  $\zeta = 2$  are engaged. Note the good performance of the compensators with the signals in phase with the desired reference.

When comparing the results of both values of  $\omega_n$ , it can be seen that the AW compensators for  $\zeta = 2$  produce better responses than the compensators for  $\zeta = 0.5$ .

Since all experiments were carried out outdoors, there are some differences between all flights recorded due to weather conditions such as gust, wind speed etc.

**Remark 2:** Both the simulation tests and the experimental tests confirm that

the higher the value of  $\omega_n$  chosen, the better the performance of the AW compensator at different  $\zeta$ . However, it is important to note that the choice of  $\omega_n$  should be such that the AW compensator is sufficiently fast enough to give good performance but within the limit of the quadrotor's processor power.

## 5. Conclusion

This paper has proposed a technique for synthesizing AW compensators for systems containing double integrators. A Popov-like sufficient condition from [24] was used to ensure closed-loop global stability of the system and simple linear analysis based on the compensators natural frequency and damping ratio was used to guide design of the compensator. The resulting expression for the free-parameter  $F_D$  in the anti-windup compensator is exceptionally simple and a range of values can be chosen without having to repeat any stability analysis.

This approach was used to synthesize AW compensators for a quadrotor system and applied both in simulation and on an experimental platform. The results show that during saturation, the quadrotor system performance improved and hence illustrates the effectiveness of the approach. It is not claimed that the results reported here are superior to those in [21], but the anti-windup design procedure is considerably simpler and re-design rapid.

## References

- [1] W. Ren, R. W. Beard, Consensus algorithms for double-integrator dynamics, Distributed Consensus in Multi-vehicle Cooperative Control: Theory and Applications (2008) 77–104.
- [2] G. Xie, L. Wang, Consensus control for a class of networks of dynamic agents, International Journal of Robust and Nonlinear Control 17 (10-11) (2007) 941–959.
- [3] B. Zhou, G. Duan, Z. Lin, Global stabilization of the double integrator system with saturation and delay in the input, Circuits and Systems I: Regular Papers, IEEE Transactions on 57 (6) (2010) 1371–1383.
- [4] G. Shi, A. Saberi, On the input-to-state stability (iss) of a double integrator with saturated linear control laws, in: Proceedings of the American control conference, Vol. 1, 2002, pp. 59–61.
- [5] J. M. Goncalves,  $L_2$ -gain of double integrators with saturation nonlinearity, Automatic Control, IEEE Transactions on 47 (12) (2002) 2063–2068.
- [6] C.-Y. Kao, On the  $L_2$ -gain of a double integrator with feedback loop saturation nonlinearity, Automatic Control, IEEE Transactions on 46 (3) (2001) 501–504.
- [7] L. Zaccarian, A. Teel, Modern Anti-windup Synthesis: Control Augmentation for Actuator Saturation, Princeton University Press, New Jersey, 2011.

- [8] S. Tarbouriech, G. Garcia, J. M. Gomes da Silva Jr., I. Queinnec, *Stability and Stabilization of Linear Systems with Saturating Actuators*, Springer, 2011.
- [9] A. Glattfelder, W. Schaufelberger, *Control systems with input and output constraints*, Springer, London, 2003.
- [10] S. Galeani, S. Tarbouriech, M. Turner, L. Zaccarian, A tutorial on modern anti-windup design, *Eur. J. Control* 15 (3) (2009) 418–440.
- [11] M. V. Kothare, P. J. Campo, M. Morari, C. N. Nett, A unified framework for the study of anti-windup designs, *Automatica* 30 (12) (1994) 1869–1883.
- [12] C. Edwards, I. Postlethwaite, An anti-windup scheme with closed-loop stability considerations, *Automatica* 35 (4) (1999) 761–765.
- [13] L. Zaccarian, A. R. Teel, A common framework for anti-windup, bumpless transfer and reliable designs, *Automatica* 38 (10) (2002) 1735–1744.
- [14] P. F. Weston, I. Postlethwaite, Linear conditioning for systems containing saturating actuators, *Automatica* 36 (9) (2000) 1347–1354.
- [15] G. Grimm, J. Hatfield, I. Postlethwaite, A. R. Teel, M. C. Turner, L. Zaccarian, Anti-windup for stable linear systems with input saturation: an lmi-based synthesis, *Automatic Control, IEEE Trans.* 48 (9) (2003) 1509–1525.
- [16] M. C. Turner, I. Postlethwaite, Further results on full-order anti-windup synthesis: exploiting the stability multiplier, *Nonlinear Control Systems 2004* 1.
- [17] S. Tarbouriech, I. Queinnec, G. Garcia, Stability region enlargement through anti-windup strategy for linear systems with dynamics restricted actuator, *Int. J. Systems Science* 37 (2) (2006) 79–90.
- [18] J. Sofrony, M. C. Turner, I. Postlethwaite, Anti-windup synthesis using riccati equations, *Int. J. Control* 80 (1) (2007) 112–128.
- [19] J.-M. Biannic, S. Tarbouriech, Optimisation and implementation of dynamic anti-windup compensators with multiple saturations in flight control systems, *Control Eng Pract* 17 (6) (2009) 703–717.
- [20] N. A. Ofodile, M. C. Turner, O. C. Ubadike, Channel-by-channel anti-windup design for a class of multivariable systems, in: *American Control Conference (ACC)*, 2015.
- [21] N. A. Ofodile, M. C. Turner, Decentralized approaches to antiwindup design with application to quadrotor unmanned aerial vehicles, *IEEE Transactions on Control Systems Technology* Volume:PP (Issue: 99) (2016) 1 – 13.
- [22] G. Herrmann, M. C. Turner, I. Postlethwaite, Discrete-time and sampled-data anti-windup synthesis: stability and performance, *Int. J. Systems Science* 37 (2) (2006) 91–113.
- [23] P. M. Dower, C. M. Kellett, H. Zhang, A weak  $L_2$ -gain property for nonlinear systems, in: *Decision and Control (CDC), 2012 IEEE 51st Annual Conference on, IEEE*, 2012, pp. 2286–2291.

- [24] F. Tyan, D. S. Bernstein, et al., Global stabilization of systems containing a double integrator using a saturated linear controller, *Int. J. Rob. and Nonlinear Contr.* 9 (15) (1999) 1143–1156.
- [25] A. A. Adegbege, W. P. Heath, Directionality compensation for linear multivariable anti-windup synthesis., *Int. J. Control* 88 (11) (2015) 2392–2402.
- [26] N. A. Ofodile, M. C. Turner, J. Sofrony, Alternative approach to anti-windup synthesis for double integrator systems, in: *American Control Conference (ACC)*, 2016, IEEE, 2016, pp. 5473–5478.
- [27] R. C. Leishman, J. Macdonald, R. W. Beard, T. W. McLain, Quadrotors & accelerometers.
- [28] S. Bouabdallah, P. Murrieri, R. Siegwart, Design and control of an indoor micro quadrotor, in: *Robotics and Automation, 2004. Proceedings. ICRA'04. 2004 IEEE International Conference on*, Vol. 5, IEEE, 2004, pp. 4393–4398.
- [29] S. Bouabdallah, R. Siegwart, Full control of a quadrotor, in: *Intelligent robots and systems, 2007. IROS 2007. IEEE/RSJ international conference on*, IEEE, 2007, pp. 153–158.
- [30] W. Ren, R. W. Beard, CLF-based tracking control for UAV kinematic models with saturation constraints, in: *Decision and Control, 2003. Proceedings. 42nd IEEE Conference on*, Vol. 4, IEEE, 2003, pp. 3924–3929.
- [31] N. Kahveci, P. Ioannou, M. Mirmirani, Adaptive LQ control with anti-windup augmentation to optimize UAV performance in autonomous soaring applications, *IEEE Trans. on Control Systems Technology* 16 (4) (2008) 691–707.
- [32] O. Falkenberg, J. Witt, U. Pilz, U. Weltin, H. Werner, Model identification and H-infinity attitude control for quadrotor MAV's, *Intelligent Robotics and Applications* 7507 (2012) 460–471.
- [33] UnmannedTech.co.uk. 2014 3DR Quad Kit [online] (2014).
- [34] R. W. Beard, Quadrotor dynamics and control, Brigham Young University.